Logarithmic Growth of AlN_x Barriers in $Nb/Al–AlN_x/Nb$ Tunnel Junctions

Akira Endo, Takashi Noguchi, Matthias Kroug, and Tomonori Tamura

***Abstract*—The growth rate of ultra-thin AlN_x films during low energy plasma nitridation has been studied by measuring the normal state resistance-area product (R_NA) of $Nb/Al–AlN_x/Nb$ Superconductor-Insulator-Superconductor junctions. The barriers were formed by nitridizing the surface of Al films with an rf plasma discharge of N_2 gas diluted to 10% with He. The reaction was started smoothly by adopting a "two-step-ignition" technique. Junctions with $R_NA = 10^0$–10^6 $\Omega\cdot\mu m^2$ were fabricated by this process. A power law relationship between R_NA and nitridation time was found to hold across the whole range of the measured R_NA values. This implies that the physical thickness of the AlN_x layer obeys a logarithmic growth law.**

Index Terms—Submillimeter wave mixers, Superconducting device fabrication, Superconductor-insulator-superconductor devices

I. Introduction

Ultra-thin films of aluminum nitride (AlN_x) have been proved to serve as excellent tunnel barriers for Superconductor-Insulator-Superconductor (SIS) junctions with normal state resistance-area products (R_NA) less than 10 $\Omega\cdot\mu m^2$ [1, 2]. Such low-R_NA SIS junctions are essencial in the development of broadband and high-sensitivity SIS mixers for astronomical observations in the submillimeter-terahertz range. While classical aluminum oxide (AlO_x) barrier SIS junctions begin to suffer from large leakage current below $R_NA = 20$ $\Omega\cdot\mu m^2$, AlN_x barrier SIS junctions can have $R_NA <$ 1 $\Omega\cdot\mu m^2$ with still decent quality, e.g., $R_{sg}/R_N > 10$ [1]. This can be understood as a result of the lower barrier height of AlN_x barriers compared to AlO_x barriers ($\phi_{AlNx} < 0.9$ eV [3], $\phi_{AlOx} < 2$ eV [4]).

While there have been a number of studies reporting successful fabrication of high quality AlN_x barriers with low R_NA by rf plasma nitridation [1, 5–11], controlling the R_NA is a problem. This is because the nitridation of aluminum requires a plasma process which involves many free parameters, such as nitridation time, substrate temperature, rf power, dc voltage, N_2 pressure and flow rate, etc. The dependence of the R_NA product on these parameters has been studied by several authors [7–10, 12]. Among these parameters, the reported nitridation-time dependence of R_NA differs from one study to another. While pioneering studies applied linear fits to their data (R_NA t_N) [5, 6], subsequent studies have reported exponential relations (R_NA e^{kt_N}) [13, 14], or peculiar relations involving plateaus [8, 9]. Meanwhile, no theory has been established which predicts the growth rate of the thickness of the AlN_x layer during low energy plasma nitridation. Thus the relation between the R_NA and nitridation time has been elucidated neither experimentally nor theoretically, and therefore the search for the appropriate process parameters involves a considerable amount of trial and error.

In this work, we fabricated many $Nb/Al–AlN_x/Nb$ SIS junctions using a composite plasma of N_2 and He. By comparing their R_NA and nitridation time, we investigated the rate and mechanism of the growth of AlN_x barriers.

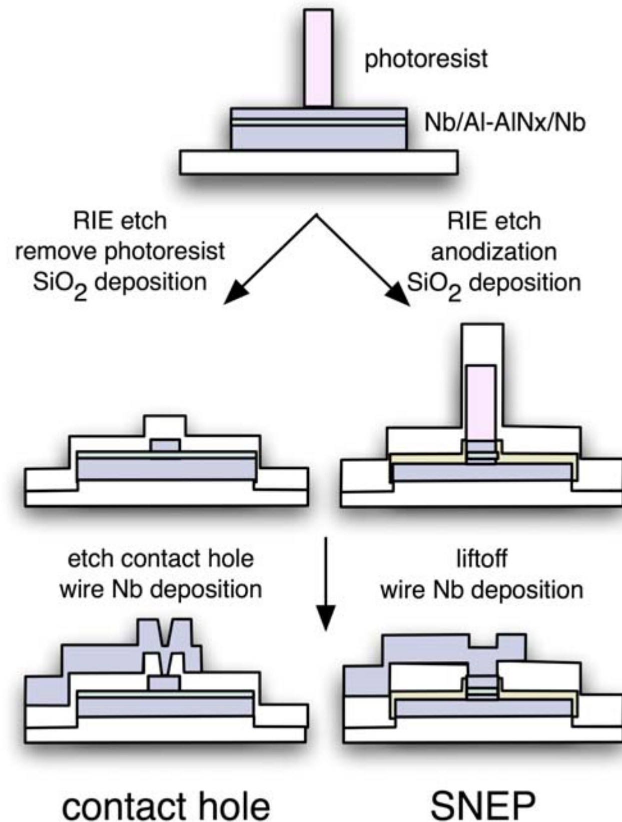

Fig. 1. Schematic diagram of the two kinds of fabrication processes.

II. Fabrication of $Nb/Al–AlN_x/Nb$ SIS Junctions

The junctions were prepared using either the standard Selective Nb Etching Process (SNEP) [15] or a contact-hole

Manuscript received May 1, 2007. This work was supported in part by the Japan Society for the Promotion of Science (JSPS) for Young Scientists.

A. Endo, T. Noguchi, M. Kroug, and T. Tamura are with the National Astronomical Observatory of Japan, Osawa 2-21-1, Mitaka, Tokyo, 181-8588, Japan (telephone: +81-422-34-3870, e-mail: akira.endo@nao.ac.jp).

A. Endo is also a JSPS research fellow at the Institute of Astronomy, University of Tokyo, 2-21-1 Osawa, Mitaka, Tokyo 181-0015, Japan.

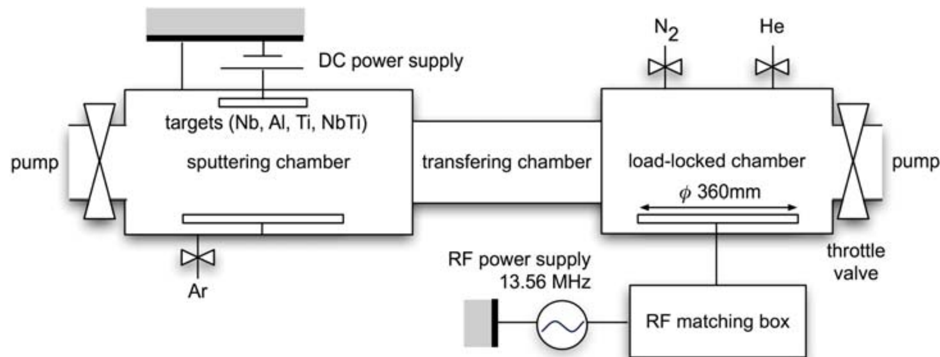

Fig. 2. Setup of the sputtering machine.

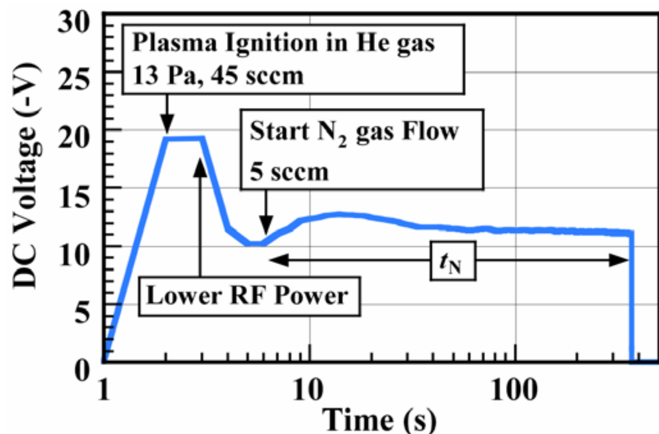

Fig. 3. DC voltage as a fuction of time during a typical nitridation process.

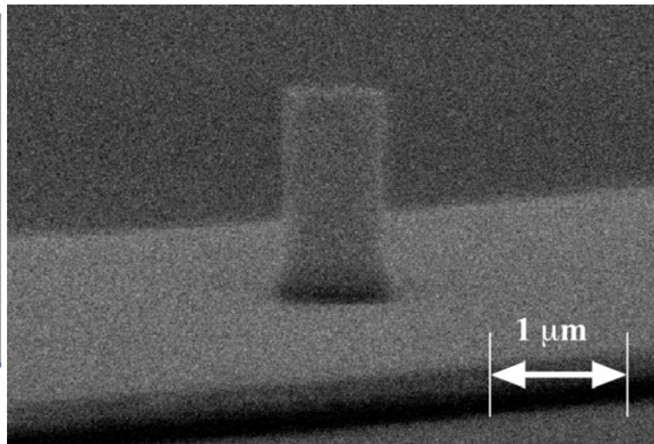

Fig. 4. SEM image of an SIS junction after RIE etching with photoresist on top. The designed diameter of the junciton was 0.8 µm.

process. The sequences of these processes are described in Fig. 1. The wafers were made of fused quartz, 35 mm in diameter and 300 µm thick. The structures of the Nb/Al–AlNx/Nb trilayers were defined by a liftoff pattern made by the Canon FPA-3000 i5+ i-line stepper. The trilayers were deposited in the ULVAC CS200 ET sputtering machine, a schematic diagram of which is presented in Fig. 2. The typical background pressure in the sputtering chamber was 1×10^{-5} Pa. The lower Nb electrode had a thickness of 200 nm and a compressive stress of 0.2–0.8 GPa. Its resistivity at room temperature was ~18 $\Omega\cdot\mu m^2$. The thickness of the Al layer was ~10 nm.

The nitridation of the Al films were performed in the load-locked chamber of the sputtering machine. The wafer was placed directly on the electrode that creates the rf discharge, so that the reactive nitrogen ions are accelerated by the dc potential and reach the wafer. The rf power during the process was kept at the lowest possible level that the generator can supply (1 W), in order to realize the slowest and softest (i.e., low energy) nitridation condition as possible. However, a larger rf power (6 W) was needed to ignite the plasma at the beginning of the process. In order to avoid any reaction that could take place during this unstable and high-energy phase, we adopted the following sequence which we call the “two-step-ignition” technique [14]:

1) Ignition of the plasma in pure He with a large power of 6 W.
2) Reduce the power to 1W which is suitable for the process.
3) Introduce nitrogen into the chamber to start the reaction.

An example of the dc voltage at the electrode as a function of time during the nitridation process is presented in Fig. 3. The nitridation time (t_N) was defined as the time from introducing nitrogen till turning off the power. Using a mixture of N_2 and He not only allows one to adopt the method mentioned above, but also enables one to control the dc voltage and the N_2 partial pressure independently by adjusting the N_2/He ratio. In other words, the density and the momentum of the nitrogen ions can be reduced simultaneously, which should benefit in realizing a slow and low energy process. The composition of N_2 was set to 10% by adjusting the flow rate of the two gases. The total pressure was 13 Pa. While we used Ar as the solvant gas in our former work [14], we used He this time to reduce any damage of the barrier caused by etching.

After the nitridation, the upper Nb electrode was deposited to a thickness of 100 nm. An example of the photoresist pattern for junction definition is presented in Fig. 4. The junctions were round and had diameters ranging from 0.4 to 4 µm. The upper Nb electrode was etched by a CF_4 + 3%O_2 plasma in an RIE etcher. The lower electrode and the Nb wire layer (400 nm) were separated by 270 nm of SiO_2.

III. Results and Discussion

A. DC I-V Characteristics

Examples of dc *I-V* curves of SIS junctions with various $R_N A$ products are presented in Fig. 5. The normal-state resistance (R_N) and the sub-gap resistance (R_{sg}) were measured at 4 and 2 mV, respectively. The leakage current began to increase at $R_N A \leq 20\ \Omega\cdot\mu m^2$, which was similar to our previous work using Ar to dilute the N_2 plasma [14]. It was also found that the optimum sputtering time for the Al layer to achieve the smallest leakage current and largest gap voltage [16] was about half of what was optimum in the previous study. We speculate that a considerable amount of Al was etched by the Ar ions during the nitridation in the previous study, which reduced the final thickness of the Al–AlN_x bilayer.

In this study, we define the term "calibrated normal-state resistance" ($R_{N,c}$) as the normal resistance after subtracting the sub-gap current portion from the dc *I-V* curve. We will refer to the $R_{N,c}A$ product rather than the nominal $R_N A$ product when we discuss the dependence of the resistivity or physical thickness of the barrier on the nitridation time, because the thickness of the barrier correlates exponentially only with the tunnel current, and not with the leakage current that goes through the pinholes.

B. Dependence of $R_{N,c}A$ on Nitridation Time

The dependence of $R_{N,c}A$ on the nitridation time is presented in the form of a log-log plot in Fig. 6, along with data collected from literature [5–8, 13, 14]. Critical current density values in literature were converted to $R_{N,c}A$ by applying the theoretical BCS relation: $J_C R_{N,c} A = \pi\Delta/2e$. Our results are well fitted by a straight line that streches across nearly six orders of magnitude in $R_{N,c}A$, which implies that there is a power law relationship between $R_{N,c}A$ and t_N as follows:

$$R_{N,c}A = 6.5 \times 10^{-6}\, t_N^{3.9}\ \Omega\cdot\mu m^2, \tag{1}$$

where t_N is the nitridation time in s. It is also possible that the experiments by previous studies presented in Fig. 6 also follow certain power laws, but were not noticed because the data was collected for no more than 3 orders of magnitude in $R_{N,c}A$. Nevertheless, if we fit every result with a power law of the form $R_{N,c}A = Ct_N^k$, we observe that the power law index k has a range of $0.5 \leq k \leq 3.9$. It is interesting that the data from our prior experiment using Ar as a solvent gas yields $k = 1.8$, which is considerably smaller compared to the He process, even though the total pressure, gas composition ratio and the applied power were kept the same. This implies that the species of the solvent gas has a significant effect on the growth rate of the AlN_x layer. It should also be noted that the process of this work is one of the slowest to approach 10 $\Omega\cdot\mu m^2$, which is favorable in controlling the $R_N A$ at this range. The growth of the physical thickness of the AlN_x layer (d_{AlNx}) can be studied by converting $R_{N,c}A$ to d_{AlNx}. The relation between $R_{N,c}A$ and the thickness of AlN_x barriers has been studied in the range of $R_N A = 1$–$1000\ \Omega\cdot\mu m^2$ for reactively sputtered AlN_x barriers [3], and is roughly

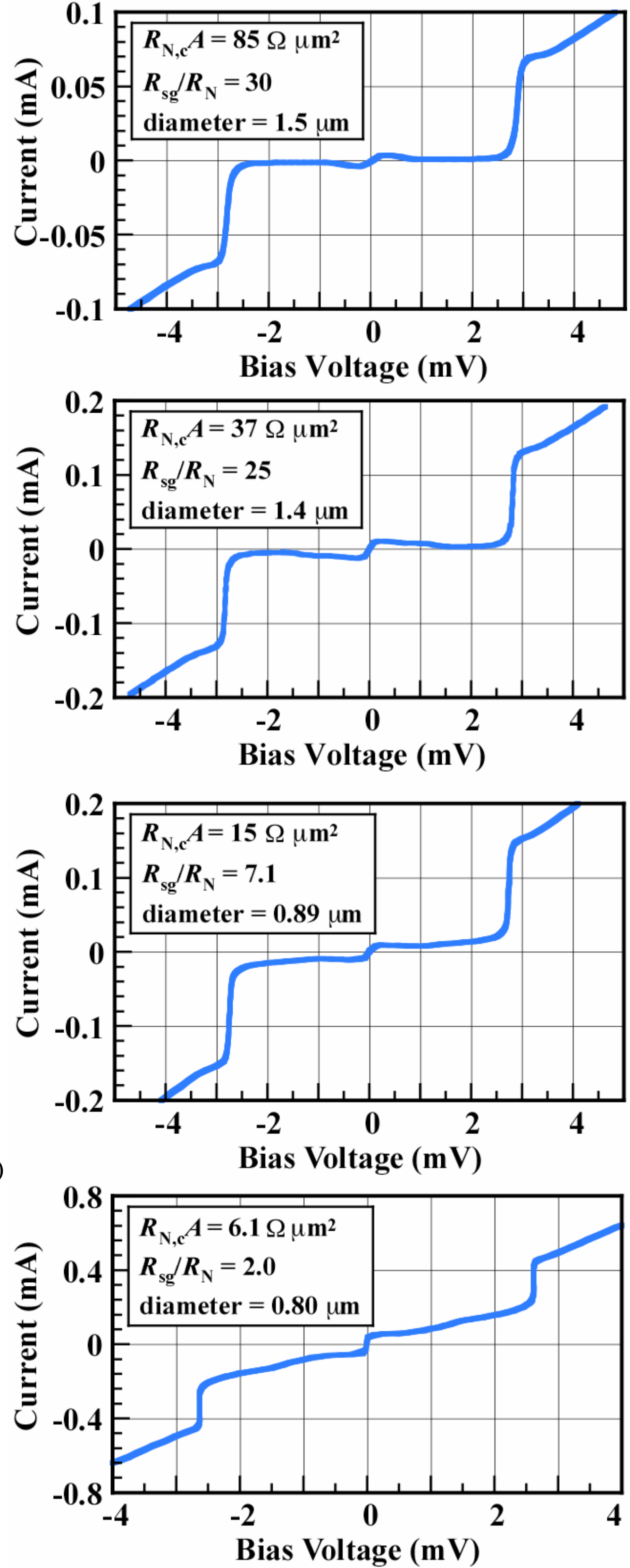

Fig. 5. DC *I-V* characteristics of junctions with various $R_{N,C}A$ products.

$$d_{AlN_x} = [0.20\log(R_{N,c}A) + 1.0]\ \text{nm}, \tag{2}$$

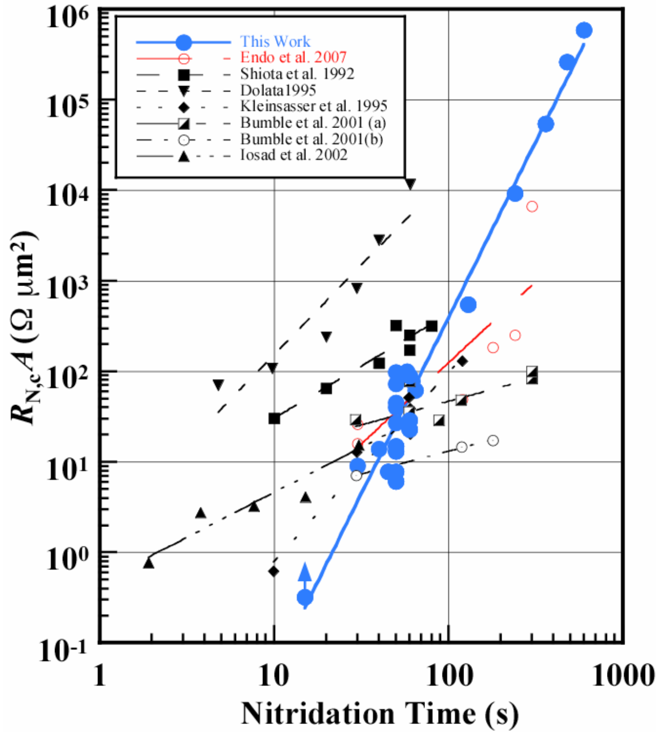

Fig. 6. Dependence of $R_{N,c}A$ on nitridation time. Data from literature are plotted together. Each data point of our data represents the average of about 20 junctions on each wafer. The arrow shows that the data point is a lower limit, for the $R_{N,c}A$ could not be sufficiently corrected for the large leakage current. The lines are least square fits to each set of data.

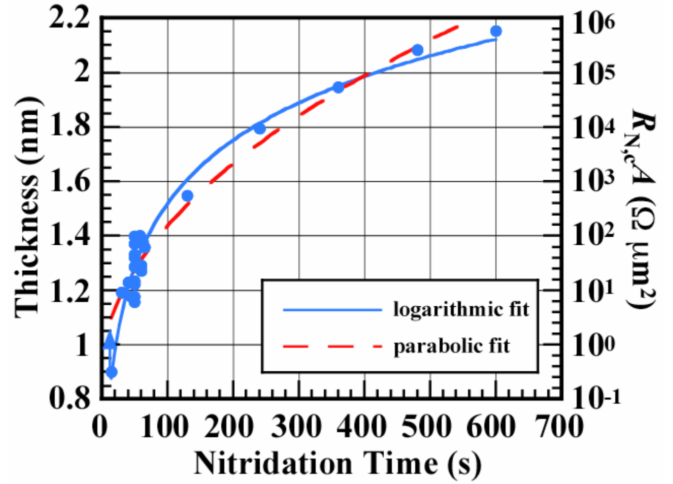

Fig. 7. Fig. 6 replotted, with the tunnel resistivity ($R_{N,c}A$) converted to the thickness of the nitride. The solid and broken curves are logarithmic and parabolic least square fits, respectively.

where $R_{N,c}A$ is in units of Ω·μm^2. If we assume that this relation holds up to $R_NA = 10^6$ Ω·μm^2, and that sputtered and plasma-nitridized AlN_x have the same barrier height, the $R_{N,c}A$ v.s. t_N relation presented in Fig. 6 can be converted into a growth curve of the AlN_x layer as shown in Fig. 7. The growth is well fitted by the following logarithmic curve, presented as a solid curve in the figure:

$$d_{AlN_x} = [0.36\log(t_N) - 0.17]\ \mathrm{nm}, \qquad (3)$$

where t_N is again in units of s. The trend of the growth curve is consistent with the growth curve observed by an in-situ ellipsometric observation [17], which observed the nitridation to saturate at a certain thickness. However, we find that the logarithmic growth continues beyond $R_NA = 10^6$ Ω·μm^2 or d_{AlNx} = 2 nm, and that it is probably difficult to realize a process in which the nitride growth completely stops at the range of our interest: $R_NA \sim 10^1$ Ω·μm^2.

Finally, we discuss the kinetics governing the growth of AlN_x barriers during low energy rf plasma nitridation. As seen in Fig. 6, we found the nitride layer to grow according to a logarithmic law. Such a behavior is observed for example when thin Al films are oxidized at room temperature or below, and is theoretically explained by migration of the metal cations [18, 19]. On the other hand, a parabolic curve (d_{AlNx} t_N) also fits our data fairly well as shown by a broken curve in Fig. 6. Such parabolic growth laws are observed in reactions with relatively high energy, for example thermal oxidation of metals at temperatures around 10^3 K, and are theoretically explained by thermal diffusion [20–22]. In fact, Iosad *et al.* [8, 9] have carefully considered the energy of various species in the nitrogen plasma, and concluded that thermal diffusion of nitrogen is the dominant mechanism in the nitridation of the Al films. They estimated the power density of the nitrogen ions reaching their substrate chuck to be 5–9 W·m^{-2} from direct Langmuir probe measurements. This value is similar to the upperlimit in our system (10 W·m^{-2}), assuming that all of the applied rf power is uniformly dissipated on the driven electrode. Though our data is marginally better fitted by a logarithmic curve, additional experiments are definitely necessary to make a conclusion on the mechanism dominating the growth of the AlN_x barriers.

IV. Conclusion

We fabricated Nb/Al–AlN_x/Nb SIS junctions by plasma nitridation of Al, using N_2 gas diluted with He. SIS junctions with decent quality can be fabricated using this process. There is a power law relationship between the R_NA and t_N that holds across $R_NA = 10^0$–10^6 Ω·μm^2. This implies that the physical thickness of the AlN_x barrier obeys a logarithmic growth law. These results will contribute to controlling the R_NA of AlN_x barrier SIS junctions.

Acknowledgment

A. Endo thanks Shin'ichiro Asayama, Yoshinori Uzawa, and Wenlei Shan for technical advice and helpful discussions.

References

[1] M. Y. Torgashin, V. P. Koshelets, P. N. Dmitriev, A. B. Ermakov, L. V. Filippenko, and P. A. Yagoubov, *IEEE Trans. on Appl. Supercond.* 17 (2007), to be published.

[2] C. F. J. Lodewijk, T. Zijlstra, D. N. Loudkov, T. M. Klapwijk, F. P. Mena, and A. M. Baryshev, *Proc. of the 18th Int. Symp. on Space THz Tech.* (2007), to be published.

[3] Z. Wang, H. Terai, A. Kawakami, and Y. Uzawa, *Appl. Phys. Lett.* 75, 701 (1999).

[4] S. Tolpygo, E. Cimpoiasu, X.Liu, N. B. Simonian, Y. A. Polyakov, J. E. Lukens, and K. K. Likharev, *IEEE Trans. Appl. Supercond.* 13, 99 (2003).

[5] T. Shiota, T. Imamura, and S. Hasuo, *Appl. Phys. Lett.* 61, 1228 (1992).

[6] A. Kleinsasser, W. Mallison, and R. Miller, *IEEE Trans. Appl. Supercond.* 5, 2318 (1995).

[7] B. Bumble, H. G. LeDuc, and J. A. Stern, *Proc. of the 9th Int. Symp. on Space THz Tech.* pp. 295–304 (2001).

[8] N. N. Iosad, A. B. Ermakov, F. E. Meijer, B. D. Jackson, and T. M. Klapwijk, *Supercond. Sci. Tech*. 15, 945 (2002).

[9] N. N. Iosad, M. Kroug, T. Zijlstra, A. B. Ermakov, B. D. Jackson, M. Zuiddam, F. E. Meijer, and T. M. Klapwijk, *IEEE Trans. Appl. Supercond*. 13, 127 (2003).

[10] P. N. Dmitriev, I. L. Lapitskaya, V. Filippenko, A. B. Ermakov, S. V. Shitov, G. V. Prokopenko, S. A. Kovtonyuk, and V. P. Koshelets, *IEEE Trans. Appl. Supercond.* 13, 107 (2003).

[11] M. J. Wang, *Proc. of the 5th Workshop on Submillimeter-Wave Reciever Technologies in Eastern Asia* p. 91 (2004).

[12] B. Bumble, H. G. LeDuc, J. A. Stern, and K. G. Megerian, *IEEE Trans. Appl. Supercond.* 11, 76 (2001).

[13] R. Dolata, M. Neuhaus, and W. Jutzi, *Physica C* 241, 25 (1995).

[14] A. Endo, T. Noguchi, T. Matsunaga, and T. Tamura, *IEEE Trans. Appl. Supercond.* 17 (2007), to be published.

[15] M. Gurvitch, M. A. Washington, and H. A. Huggins, *Appl. Phys. Lett*. 42, 472 (1983).

[16] T. Imamura and S. Hasuo, *J. Appl. Phys*. 66, 2173 (1989).

[17] T. W. Cecil, R. M. Weikle, A. R. Kerr, and A. W. Lichtenberger, *IEEE Trans. Appl. Supercond*. 17 (2007), to be published.

[18] N. Cabrera and N. F. Mott, *Rep. Prog. Phys*. 12, 163 (1948).

[19] F. P. Fehlner and N. F. Mott, *Oxidation of Metals* 2, 59 (1970).

[20] B. E. Deal and A. S. Grove, *Journal of Applied Physics* 36, 3770 (1965).

[21] C. Wagner, *Corrosion Science* 9, 91 (1969).

[22] R. H. Doremus, *J. Appl. Phys*. 95, 3217 (2004).